Journal of Molecular Histology (2025) 56:129
https://doi.org/10.1007/s10735-024-10324-z

ORIGINAL PAPER

PBK as a novel biomarker performed excellent diagnostic and prognostic value in HCC associated with immune infiltration and methylation

Beibei Lv[1] · Fenna Zhang[1] · Xinyi Zhang[1,2] · Ziyi Wang[1,2] · Shuai Hao[1,2] · Na Ye[1] · Na He[1]

Received: 15 August 2024 / Accepted: 27 November 2024 / Published online: 3 April 2025

Abstract

Diagnostic and prognosis of hepatocellular carcinoma (HCC) remain major challenge in clinic. This study aimed to explore a gene signature for diagnosis and prognosis prediction of HCC followed by mechanism investigation. Differentially expressed genes (DEGs) in HCC were screened using TCGA. With specific formula, clinic features of prognosis associated DEGs were calculated to obtained a specific model followed by Kaplan–Meier analysis. Protein–protein interaction (PPI) were predicted using STRING and associations between hub gene and clinic features were analyzed using R software. The hub gene was silenced in HCC cell lines followed by cell behaviors analyses. A prognosis associated 14-gene model was identified in this study which could significantly distinguish samples into high-risk and low-risk groups. PBK, BUB1, NUF2, and CDCA8 were the key nodes involved in the 14 gene-coded PPI with high diagnostic values, and only PBK was an independent risk factor of disease specific survival (DSS) of HCC. Moreover, higher PBK was positively correlated with pathological and histological grades, higher AFP, and infiltrations of Th2, T helper cells and aDC of HCC, but negatively correlated with the killer immune cells. Dysregulated methylation might contribute to the higher expression of PBK and silencing PBK significantly suppressed the proliferation, growth, migration, and invasion of HCC cells. PBK, BUB1, NUF2, and CDCA8 played crucial role in prognosis associated 14-gene model with high diagnostic values. Methylation dysregulation-induced PBK accumulation might promote the development of HCC via modulating immune surveillance.

Keywords Hepatocellular carcinoma · PBK · Prognosis · Methylation · Immune infiltration

Introduction

In mainland of China, primary liver cancer has surpassed gastric cancer as the second leading cause of cancer related mortality (Cao et al. 2021a). Specifically, hepatocellular carcinoma (HCC) is the main histotypes of primary liver cancer, accounts for 75–85% of overall (Lin et al. 2022). Owing to the lack of manifestations in the early stage, HCC is usually detected at the advanced stage, which is largely limited the application of traditions therapies, including surgical resection, radio-frequency ablation, trans-arterial chemoembolization, liver transplantation et al. (Vogel et al. 2021). Tyrosine kinase inhibitors (TKIs) and immune checkpoint inhibitors provide new choices for treatment recently, but the outcome remains not satisfied due to the high heterogeneity among patients (Ruf et al. 2021). According to the SEER database, 5-year survival rate of HCC is only 19.6% in average and 2.5% for advanced metastatic individuals (Chidambaranathan-Reghupaty et al. 2021). Regrettably, this data in China is more dismal—less than 12.5% (Wang and Wei 2020). Hence, there remains a long way and much work to improve the prognosis of liver cancer patients.

According to the literatures, poor prognosis of HCC might attribute to the deficiency of surveillance and insufficient early diagnostic strategy. Imaging and alpha-fetoprotein test are the most frequently-used methods for HCC detection, but the high cost and low efficiency are

Beibei Lv and Fenna Zhang contributed equally to this work.

✉ Na Ye
270954990@qq.com

✉ Na He
Hena@xiyi.edu.cn; ylhena@163.com

[1] The First Affiliated Hospital of Xi'an Medical University, Fenggao Western Road 48#, Lianhu District, Xi'an, China

[2] Office of Graduate Student Affairs, Xi'an Medical University, Han Guang North Road 74#, Beilin District, Xi'an, China

two obstacles limited their application and popularization in clinic (Chalikonda et al. 2022). With the development of sequencing and bioinformatics, cancer associated biomarkers widely explored and used to facilitate the cancer screening benefited from the noninvasive and easily accessible, including mRNAs, lncRNA, miRNAs, circRNAs, proteins, and exosomes (Debes et al. 2021; Zhao et al. 2021; Sorop et al. 2021). Although these biomarkers have been reported to play critical roles in the diagnosis and prognosis of HCC, there remains no effective candidates been successfully applied in clinic due to complex of different clinical issues.

As it widely accepted, HCC is a highly heterogeneity tumors, which can be triggered by chronic hepatitis virus B/C infection, alcohol abusing, diabetic, non-alcoholic fatty liver disease (NAFLD), or aflatoxin exposure. Effective diagnostic or prognostic signatures must depend on a well-known pathological mechanism of genes in HCC. To obtain reliable gene signature, we have generated a prognosis-associated gene model in this study based on The Cancer Genome Atlas (TCGA) database followed by the function annotations and protein–protein interactions (PPI) analysis. According to the clinical significance, the key nodes involved in PPI were screened and subjected for immune infiltration and prognosis prediction and mechanism exploration. Based on these investigations, we hope to provide some insights for the diagnosis and prognosis of HCC.

Materials and methods

Data source and screening

A total of 368 HCC tumor samples and 50 para-tumor samples were downloaded from the TCGA database (UCSC Xena database, http://xena.ucsc.edu) and enrolled in this study. After standardized using the log2(count + 1) of HCC associated gene expression matrix, 60,489 transcripts were merged with the same transcripts and gene were excluded with 0 expression. As a result, 58,388 Ensembl IDs were obtained and annotated using genecode database (ftp://ftp.sanger.ac.uk/pub/gencode/Gencode_human/). Then, Ensembl ID was inverted into Symbol ID using Python and normalized using the "normalizeBetweenArrays" in limma 3.9.19 package in R Software (Ritchie et al. 2015). In addition, the clinical features of enrolled samples were also collected, including gender, age, WHO class, T, N, M. The prognosis of certain gene was confirmed using the Kaplan–Meier Plotter (http://www.kmplot.com/analysis/index.php?P=service&cancer=pancancer_mirna) which is an online tool with sources from the database of GEO, EGA, and TCGA.

Analysis of differentially expressed genes (DEGs)

Expression difference between the tumor and para-tumor samples were analyzed using the t-test in limma package of R Software (version 3.10.3, http://www.bioconductor.org/packages/release/bioc/html/limma.html) and adjusted using false discovery rate (FDR) (Chumbley and Friston 2009). Then, the DECs were screened using the threshold of P adj. < 0.01 and |Log foldchange (FC)| > 2. Functional and pathways enrichment were analyzed using R package clusterProfiler according to the Gene Ontology (http://www.geneontology.org/) and Kyoto Encyclopedia of Genes and Genomes (KEGG) pathway (http://www.genome.jp/kegg).

Screening of prognosis associated genes in HCC and model construction

To explore the association between DEGs and prognosis of HCC, COX analysis in Survival package (Version 3.10.3, http://www.bioconductor.org/packages/release/bioc/html/survival.html) (Pohar and Stare 2006) of R was used for the single factor analysis to screen HCC associated high expressed genes. In addition, multiple test P value, namely P value = 0.05/count, was used in this analysis to reduce false positive rate and obtain more exact result (Ruppert et al. 2007). The survival associated genes, screened by single factor analysis, were subjected for Cox proportional regression of risk to construct an independent prognostic model using the least absolute shrinkage and selection operator (LASSO) algorithm (Bian et al. 2024; Gui et al. 2024). The feature value (Eigenvalues) of each sample was calculated using the formula:

$$Eigen\ values = \sum_{i=1}^{n} (coeff_i * Count)$$

n represents total gene number, $coeffi$ represents the model coefficient of i gene, count represents the gene expression.

According to the median of feature value, the enrolled genes were divided into high-risk group and low-risk group. Then, survival package (version3.2–10, http://www.bioconductor.org/packages/release/bioc/html/survival.html) in R software was utilized to analyze the association between the screen genes and prognosis. In addition, datasets of GSE54236 (Villa et al. 2016) and GSE76427 (Grinchuk et al. 2018) were downloaded from Gene Expression Omnibus database (GEO; https://www.ncbi.nlm.nih.gov/geo/) for further validation of this gene model according the aforementioned methods.

Gene set enrichment analysis (GSEA)

According to the prognosis model, genes were divided into the high-risk group and low-risk group. Then, the HALLMARK gene set (h.all.v7.4.symbols.gmt) and GO dataset (c5.go.v7.4.symbols.gmt) were used for GESA analyssis of all genes in the two groups using GSEA (v-4.1.0, http://www.gsea-msigdb.org/gsea/index.jsp).

Construction of protein–protein interaction network and functional enrichment

To explore the interaction among the prognosis associated genes, STRING (version 9.1, https://www.string-db.org) was used to construct the PPI network with the interaction score threshold ≥ 0.9. The network was visualized using cytoscape (version 3.8.2, https://github.com/cytoscape/cytoscape.js/tree/v3.8.2). Following this, the biological process in Gene Ontology (GO) of proteins were annotated using DAVID on-line database (https://david.ncifcrf.gov/).

Hub proteins expression and clinical significance

According to the PPI network and enrichment, the hub protein in this network was screened. Then, the expression of hub proteins was screened from DEGs as aforementioned and visualized using the ggplot2 package (v3.3.3) in R. The diagnostic value of proteins in HCC was assessed using the receiver operating characteristic (ROC) curve with area under the curve (AUC) using the pROC package (v1.17.0.1) and ggplot2 package (v3.3.3). Correlations between gene and survival outcomes in HCC were assessed using the survival (v3.3.1) and survminer (v0.4.9) packages followed by ggplot2 package (v3.3.3) visualization.

Correlations between gene expression and clinical features, including age, gender, T/N/M stage, pathological stage, histological stage, AFP, Child–Pugh grade, and vascular invasion were assessed using the ANOVA in the stats (v4.2.1) and car (v3.1–0) packages followed by ggplot2 package (v3.3.3) visualization. Association between gene and immune infiltration was determined using the ssGSEA in GSVA (v1.46.0) and visualized using ggplot2 package (v3.3.3). Time-dependent survival ROC and nomogram, including PBK, T, N, and M, were performed to predict the probability of 1, 3, 5-year OS in HCC using the timeROC (v0.4) followed by ggplot2 package (v3.3.3) visualization.

Methylation prediction and outcome association analysis

Methylation site of PDZ-binding kinase (PBK) was predicted using the MethSur (https://biit.cs.ut.ee/methsurv/) online tools. Following this, the survival outcomes of the significant different sites were also analyzed using the Kaplan–Meier. In addition, the expression correlations between PBK and methylation associated genes were assessed using the Spearman analysis and visualized using ggplot2 package (v3.3.3).

Clinical samples collection and detection

For further confirmation, a total of 31 cases HCC and adjacent tissue samples were enrolled from the First Affiliated Hospital of Xi′an Medical University between Dec. 2023 to Nov. 2024. The enrollment criteria were set as: (1) diagnosed as primary HCC by biopsy, (2) first diagnosed without any treatment, (3) clinical information, including age, gender, tumor stage, and metastatic status. Patients who had suffered with hereditary HCC, liver hypoplasia, other primary cancers, or another severe organ dysfunction were excluded. This study was authorized by the ethic committee of The First Affiliated Hospital of Xi′an Medical University (XYYFYLL-KTSB-2023–15). After collection, expression of PBK was detected using the quantitative real time PCR (qRT-PCR) and relative expression of PBK in HCC was calculated with the adjacent tissues as the control group.

Cell culture and lentivirus infection

Human embryonic kidney cell (HEK293T), liver stellate cell (HSC), and HCC cell lines (HLE and HCCLM3) were purchased from the Cell Bank in Chinese Academy of Sciences (Shanghai, China). HCC cell lines: hep3B, huh-7, and hepG2 were purchased from the Wuhan Pricella Biotechnology Co., Ltd (Wuhan, Hubei, China). All cells were cultured in Dulbecco's modified Eagle's medium (DMEM, Basal Media, Shanghai, China) supplemented with 10% fetal bovine serum (FBS, Basal Media) and 1% penicillin–streptomycin solution (BIO Basic lnc, Shanghai, China) in a humidity incubator at 37 °C with 5% CO_2 in atmosphere.

PBK specific lentivirus plasmids were purchased from the Applied Biological Materials (GenePharma, Shanghai, China). For lentivirus generation, HEK293T cells were transfected with the lentiviral vector and packaging plasmids by lipofectamine 2000 (Invitrogen, Carlsbad, CA, USA) according to the manufacturer's instruction. After 48 h transfection, the viral supernatants were collected, centrifuged at 75,000 g for 90 min, resuspended, and filtered by 0.45 μm filters (Millipore, Billerica, MA, USA). Then, the freshly plated HepG2 and Huh-7 were infected with the lentivirus and the knockdown efficiency was determined using qRT-PCR and western blotting after 48 h infection.

Cell proliferation assay

Cell proliferation was assessed using the Cell Counting Kit-8 (CCK-8; Beyotime, Shanghai, China) and colony formation assays. For CCK-8, cells were seeded into 96-well plates at a density of 1.0×10^4 per well and maintained for 0, 24, 48, and 72 h. After culturing, 10 µl CCK-8 reagent was added to each well and cultured for 2 h. Subsequently, the optical density of each well at 450 nm was determined using a microplate reader (Thermo, Boston, USA).

For colony assay, cells with different treatments were seeded into 6-cm plate at a density of 3.0×10^3 per well and kept for 14 days. Then, cells were fixed with 4% methanol (PFA; Sangon, Shanghai, China) and stained with 0.1% crystal violet (Sangon). Finally, the colony was photographed and the colony number was counted.

Transwell assay

Cell migration ability was assessed using the transwell assay. Briefly, cells were collected and resuspended in serum-free DMEM. Then, 1×10^4 cells in 400 µl was seeded into each 24-well transwell chamber with or without coating with Matrigel (Corning, NY, USA) and 600 µl of DMEM contained with 10% FBS was added to the lower chamber. After 48 culturing, cells on the upper chamber were scraped with a swab, fixed with 4% PFA for 30 min and stained with 0.1% crystal violet (Sangon) for 20 min at room temperature. Then, the results were captured and counted under an inverted microscope (Olympus, Japan) at the magnification of 40×.

qRT-PCR

Total RNA was isolated from tissue or cell samples using the TRIzol reagent (Takara, Dalian, Liaoning, China) according to the manufacturer's protocol. With total RNA as the template, the complementary DNA was synthesized using the M-MLV Reverse Transcriptase Kit (Takara) according to the manufacturer's instruction. Following this, qRT-PCR was performed using the SYBR qPCR Master Mix (Vazyme, Nanjing, China) on an ABI 7500 (Applied Biosystems, Foster City, CA, USA). The relative expression of curtained gene was calculated using the $2^{-\Delta\Delta Ct}$ method. Primers used for qRT-PCR were listed as follows: PBK, forward 5′-AGGTACTTGGCCACGACT TA-3′ and reverse 5′-GCCACTCTCAGTCCAGAGTC-3′; and GAPDH, forward 5′-CCACTAGGCGCTCACTGTT-3′ and reverse 5′-CCCAATACGACCAAATCCGTT-3′.

Western blotting

Protein in cell samples were extracted using the radioimmunoprecipitation assay (RIPA) buffer (Beyotime) and quantified using the BCA method (Pierce, USA). Then, 20 µg of each sample was subjected to the SDS-PAGE and electronic transferred onto PVDF membrane. After blocking with 5% non-fat milk at room temperature for 1 h, membrane was incubated with anti-PBK (1:1000 dilution; #ab280209, Abcam, Cambridge, MA, USA) and anti-GAPDH (1:5000 dilution; #ab8245, Abcam) primary antibodies at room temperature for 1 h. Next, the membrane was incubated with rabbit anti-mouse secondary antibody (1:10,000 dilution; #ab6728, Abcam) at room temperature for 1 h. Protein bands on the membrane were visualized using the enhanced chemiluminescence (ECL) method (Pierce).

Statistical analyses

Data in this study was presented with mean ± standard deviation and analyzed using GraphPad Prism 7.0 (GraphPad Software Inc., La Jolla, CA, USA). Comparisons among groups were estimated using Student t-test or one-way analysis of variance (ANOVA) followed by Turkey's test. $P < 0.05$ was considered statistical significance.

Results

Screening and function annotation of DEGs between tumor and non-tumor tissues in HCC

After quality control, a total of 418 cases of TCGA expression matrix enrolled in this study, which included 58,388 genes and 7 clinical features: WHO stage, gender, age, T, N, M, Tumor Stage. With thresholds of $|logFC| > 2$ and P adj. < 0.01, a total of 419 upregulated genes and 972 downregulated genes in tumor tissues compared with the non-tumor tissues (Fig. 1A). To get an over review, heatmap of the TOP50 upregulated and downregulated genes were depicted. The results presented no obvious color difference between the normal and tumor tissues among the TOP50 downregulated DEGs, but the TOP50 upregulated DEGs in the tumor tissues were markedly higher than that in the normal group (Fig. 1B).

According to the heatmap clustering, the 419 upregulated DEGs were subjected to the GO and KEGG analyses. GO functional enrichment analysis presented that the upregulated DEGs were significantly enriched in organelle fission, nuclear division, chromosome segregation, mitotic nuclear division, *et al.* (Fig. 1C). In addition, KEGG pathway enrichment analysis showed that the upregulated genes were significantly enriched in cell cycle, oocyte meiosis, cellular

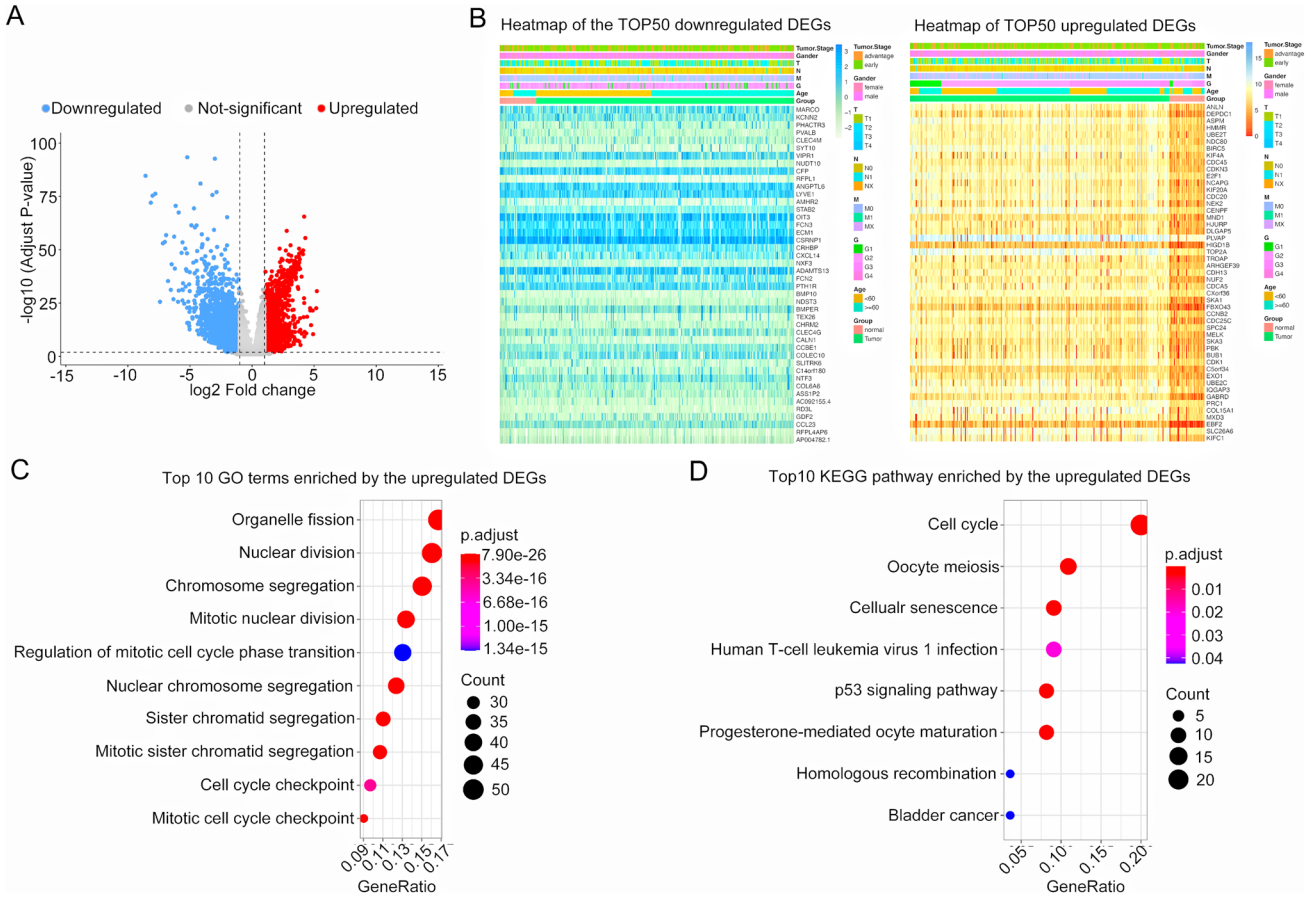

Fig. 1 DEGs screening in HCC based on TCGA database. A, The differentially expressed genes in HCC. B, Heatmaps of the top50 downregulated (left panel) and upregulated (right panel) DEGs. C, GO functional enrichment of the upregulated DEGs. D, KEGG pathway enrichment of the upregulated DEGs. DEGs, differentially expressed genes; HCC, hepatocellular carcinoma; GO, gene ontology; KEGG, Kyoto Encyclopedia of Genes and Genomes

senescence, human T-cell leukemia virus 1 infection, p53 signaling pathway, *et al* (Fig. 1D).

Prognostic signature model construction and functional enrichment analyses

To explore prognosis associated markers, the 419 upregulated DEGs were enrolled for univariate risk proportional regression analysis according the prognosis data in TCGA and 45 DEGs were associated with the prognosis of HCC (P value < 0.000119 (0.05/419)). Then, the screen 45 upregulated DEGs were enrolled for a multivariate Cox analysis to obtain overall survival (OS)-associated risk gene model. As result, a total of 14 upregulated DEGs were enrolled in this model, including *TRIP13*, *KIF4A*, *CENPA*, *CDCA8*, *CTSV*, *NUF2*, *SGO2*, *PBK*, *BUB1*, *CBX2*, *UBE2C*, *IQGAP3*, *CDCA2*, and *KIF18B* (Supplementary Table 1). According to the prognostic signature median = 5.752 in this model, 368 cases were divided into the low-risk (n = 184) and high-risk (n = 184) groups. Then, the prognosis of two groups was compared using the K-M analysis, and the results presented that the high-risk group presented a poor prognosis than the low-risk group ($P < 0.000$, Fig. 2A–C). In addition, data of GSE54236 and GSE76427 were validated that patients with higher signature score in the high-risk group presented a poor OS prognosis than patients in the low-risk group ($P < 0.001$, Fig. 2D). These results suggested that this model was stable for the prediction of HCC prognosis.

Furthermore, GESA analysis was also performed to explore mechanism alterations between the high-risk and low-risk according to this 14-gene signature. GSEA enrichment of high-risk group was significantly enriched in the upregulations of PI3K/Akt/mTOR signaling pathway, inflammatory response, IL-6/JAK/STAT3, and TNF-α/NF-κB pathway (Fig. 2E and supplementary Fig. 1A), suggested that the high-risk group was significantly with the dysregulated inflammation and cell growth and proliferation. In addition, low-risk group was markedly enriched in the downregulation of oxidative phosphorylation, bile acid metabolism, fatty acid metabolism,

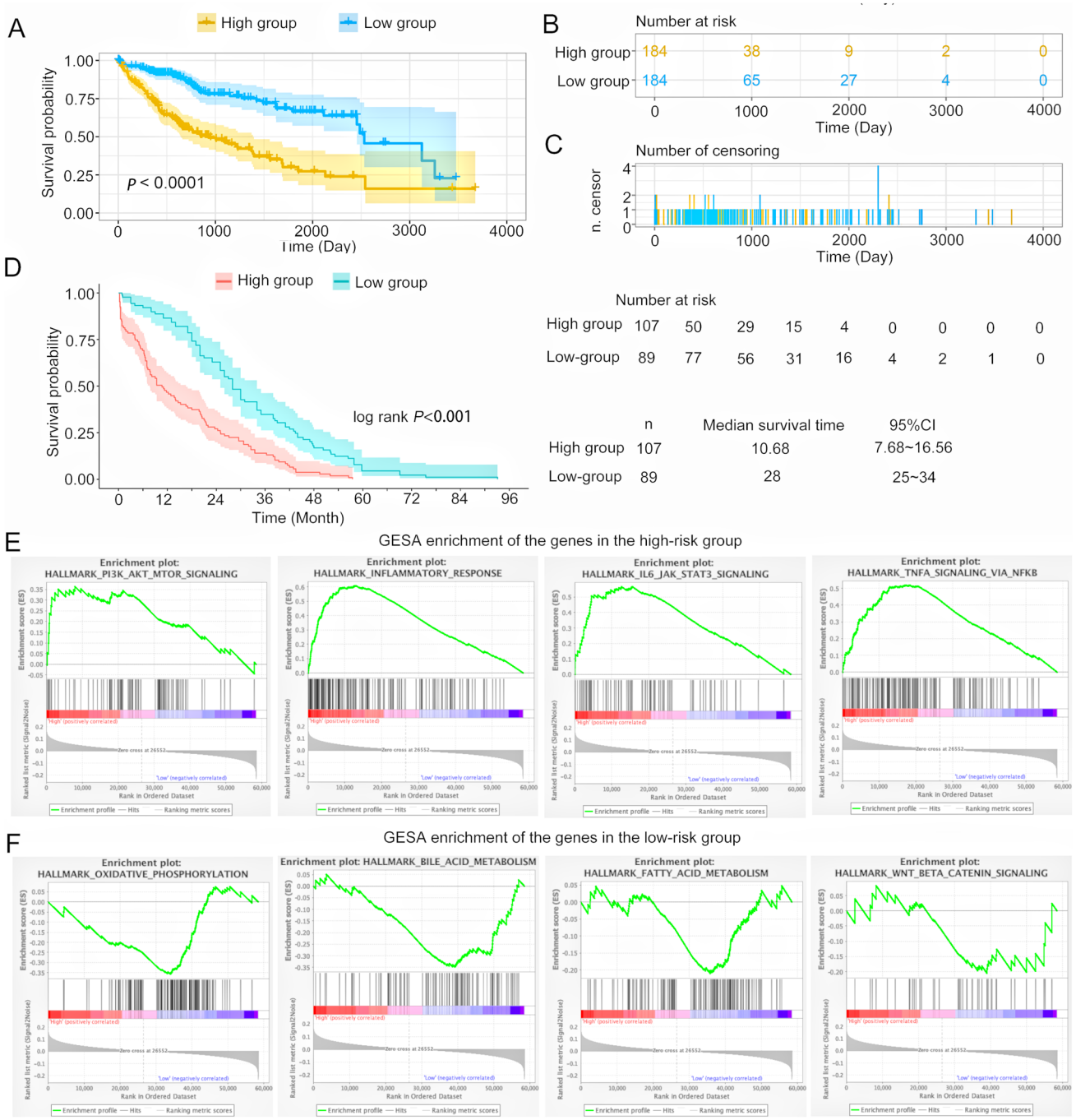

Fig. 2 A small interacted model was identified to predict the prognosis of HCC. A, The prognosis of patients in the higher risk group and lower risk group divided by the clinical feature median value. B, The sample number in each group at different time point. C, The number of censors in different group at different time point. D, The prognosis of patients in the higher risk group and lower risk group validated in GSE54236 and GSE76427 datasets. E, The GESA enrichment of genes involved in the high-risk group; F, The GESA enrichment of genes involved in the low-risk group. HCC, hepatocellular carcinoma; GESA, Gene Set Enrichment Analysis; CI, confidential interval

and Wnt/β-catenin signaling pathway (Fig. 2F and supplementary Fig. 1B), suggesting that the downregulation of lipid metabolism disorder and its associated oxidative phosphorylation might presented lower risk for prognosis.

PBK, CDCA8, BUB1, and NUF2 played critical roles in PPI network

To further explore the correlations among these 14 genes,

the interactions among these genes coded proteins were also analyzed according to the STRING database. A total of 25 interaction pairs were identified with the threshold of interaction score ≥ 0.9. This model presented that these proteins were tightly interacted with others, except CTSV, IQGAP3, and TRIP13 (Fig. 3A), suggested a relative integrality among them.

For further analysis, GO-BP functional enrichment was performed to reveal the biofunction of this network. The results suggested that proteins in PPI were significantly enriched in the mitotic sister chromatid segregation, indicating that proteins in this model were significantly correlated with cell proliferation, which was markedly in accordance with the feature of HCC (Table 1). Specifically, PBK and CDCA8 were significantly enriched in cell cycle checkpoint, and BUB1 and NUF2 were significantly enriched in the mitotic spindle assembly checkpoint signaling, suggesting that PBK, CDCA8, BUB1, and NUF2 might play critical roles in the origination of cell proliferation.

According to these findings, the expression of PBK, CDCA8, BUB1, and NUF2 were determined and identified that all of them were significantly upregulated in the HCC compared with the normal samples whether matched nor not (Fig. 3Band C). Then, the diagnostic and prognostic values of PBK, CDCA8, BUB1, and NUF2 were evaluated. The results suggested that all of them performed excellent diagnostic values with AUC more than 0.96 (Fig. 3D). In addition, K-M analysis showed that the 5-year OS of patients

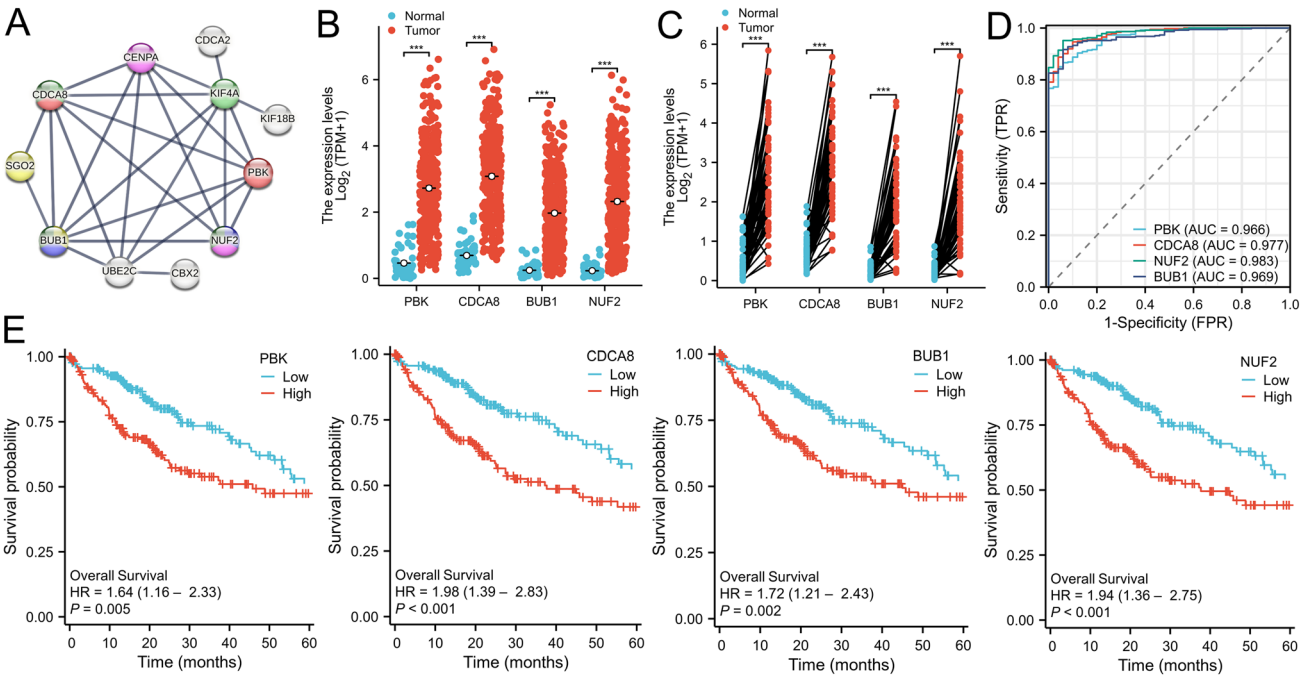

Fig. 3 PBK, CDCA8, BUB1, and NUF2 play key roles in prognosis associated gene/protein interaction network. A, Protein–protein interaction network of the proteins involved in the prognosis associated gene mode. B, Expression of PBK, CDCA8, BUB1, and NUF2 in HCC and normal controls extracted from TCGA database. C, Expression of PBK, CDCA8, BUB1, and NUF2 in matched HCC and normal controls extracted from TCGA database. D, The diagnostic values of PBK, CDCA8, BUB1, and NUF2 in HCC determined using ROC curve. E, Kaplan–Meier analyses of HCC patients with different expression of PBK, CDCA8, BUB1, and NUF2. HCC, hepatocellular carcinoma; ROC, receiver operator characteristic curve. ***$P < 0.001$

Table 1 The GO-BP enrichment of PPI network

GO-BP	Description	Strength	Protein	False discovery rate
GO:0051754	Meiotic sister chromatid cohesion, centromeric	2.75	BUB1, SGO2	0.0033
GO:0051256	Mitotic spindle midzone assembly	2.41	CDCA8, KIF4A	0.0100
GO:1,901,978	Positive regulation of cell cycle checkpoint	2.17	CDCA8, PBK	0.0223
GO:0007094	Mitotic spindle assembly checkpoint signaling	2.13	BUB1, NUF2	0.00094
GO:0051383	Kinetochore organization	2.13	NUF2, CENPA	0.0263
GO:0033047	Regulation of mitotic sister chromatid segregation	2.01	BUB1, CDCA8, NUF2	4.83×10^{-5}

with higher expression of PBK, CDCA8, BUB1, and NUF2 were significantly lower than that in the patients with lower expression (Fig. 3E). However, the cox regression analyses suggested only PBK was an independent risk factor for the DSS of patients (Table 2). Considering of this, the PBK might play key role in the HCC development and choose for the following investigation.

High PBK1 expression was correlated with the adverse clinical features and immune infiltrations of HCC

Correlations between clinical features and PBK were analyzed based on the information provided by TCGA database. The results presented that PBK expression was significantly increased in tumor samples compared with the normal controls in age, gender, T stage, N stage, M stage, tumor stage, histological stage, AFP level, Child–Pugh grade, and vascular invasion (Fig. 4A–J), which were consistent with the expression of PBK between normal and HCC samples. Additional, PBK expression was also significantly increased along with the development in T stage (Fig. 4C), tumor stage (Fig. 4F), histological stage (Fig. 4G), and AFP level (Fig. 4H) of HCC, suggesting that PBK might significantly correlated with the development of HCC. The clinical sample validations also suggested that PBK was markedly increased in HCC (Fig. 4K). Further stratification analyses showed that PBK expression was not different in age and gender, but positively correlated with the advanced tumor stage and metastasis (Fig. 4L–O). Since PBK has been reported to serve critical role in the regulations of G2/M checkpoint and immune checkpoint, which was suggested to play critical role in tumor development, correlation between PBK and immune infiltrations were assessed in the following. The results demonstrated that PBK was positively correlated with the infiltration's of Th2 cells, T helper cells, and activated dendritic cells (aDC), but negatively correlated with the B cells, immature DC (iDC), CD8 T cells, plasmacytoid DC (pDC), nature killer (NK) cells, eosinophils, mast cells, cytotoxic cells, neutrophils, DC, and Th17 cells (Fig. 4P). Based on these findings, the prediction ability of PBK was assessed in HCC with a time-dependent ROC and found that the AUCs of 1-, 3-, 5-year survival curve were all more than 0.6 (Fig. 4Q), suggesting that these data might be adequate for the survival prediction. Finally, we generated a nomogram model to predict the 1-, 3-, and 5-year survival probability of HCC by combining T, N, M stages, and PBK expression levels and found that PBK severed comparable role to N stage in the HCC survival prediction (Fig. 4R).

Methylation dysregulated PBK might promote the cell growth and metastasis of HepG2 and Huh-7

Hypermethylation is considered to be an important modification in gene expression. In this study, we had predicted all the detected methylation sites of PBK and found that cg17973772 and cg21887430 sites presented obvious color differences in the site heatmap (Fig. 5A). Thus, the prognostic outcomes of these two sites were analyzed and found that cg17973772 and cg 21,887,430 sites were significantly correlated with the OS of HCC patients (Fig. 5B). In addition, correlations of PBK and methylation associated genes suggested that PBK expression was significantly correlated with the expression of methylation readers and writers, especially RBMX and IGF2BP3 (Fig. 5C). These findings suggested

Table 2 The correlations between gene expression and survival outcome in HCC

Item	OS				DSS			
	Univariate analysis		Multivariate analysis		Univariate analysis		Multivariate analysis	
	HR (95%CI)	P value	HR (95%CI)	*P* value	HR (95%CI)	P value	HR (95%CI)	*P* value
PBK								
Low (n = 187) High (n = 186)	1.643 (1.160–2.328)	0.005	0.892 (0.501–1.586)	0.696	1.493 (0.958–2.327)	0.077	0.429 (0.222–0.828)	0.012*
CDCA8								
Low (n = 187) High (n = 186)	1.985 (1.394–2.825)	< 0.001	1.799 (0.971–3.333)	0.062	2.502 (1.571–3.985)	< 0.001	2.087 (0.934–4.663)	0.073
NUF2								
Low (n = 187) High (n = 186)	1.935 (1.362–2.749)	< 0.001	1.629 (0.882–3.008)	0.119	2.339 (1.481–3.692)	< 0.001	2.166 (0.994–4.720)	0.052
BUB1								
Low (n = 187) High (n = 186)	1.716 (1.209–2.434)	0.002	0.805 (0.410–1.578)	0.528	2.242 (1.413–3.556)	< 0.001	1.286 (0.531–3.113)	0.578

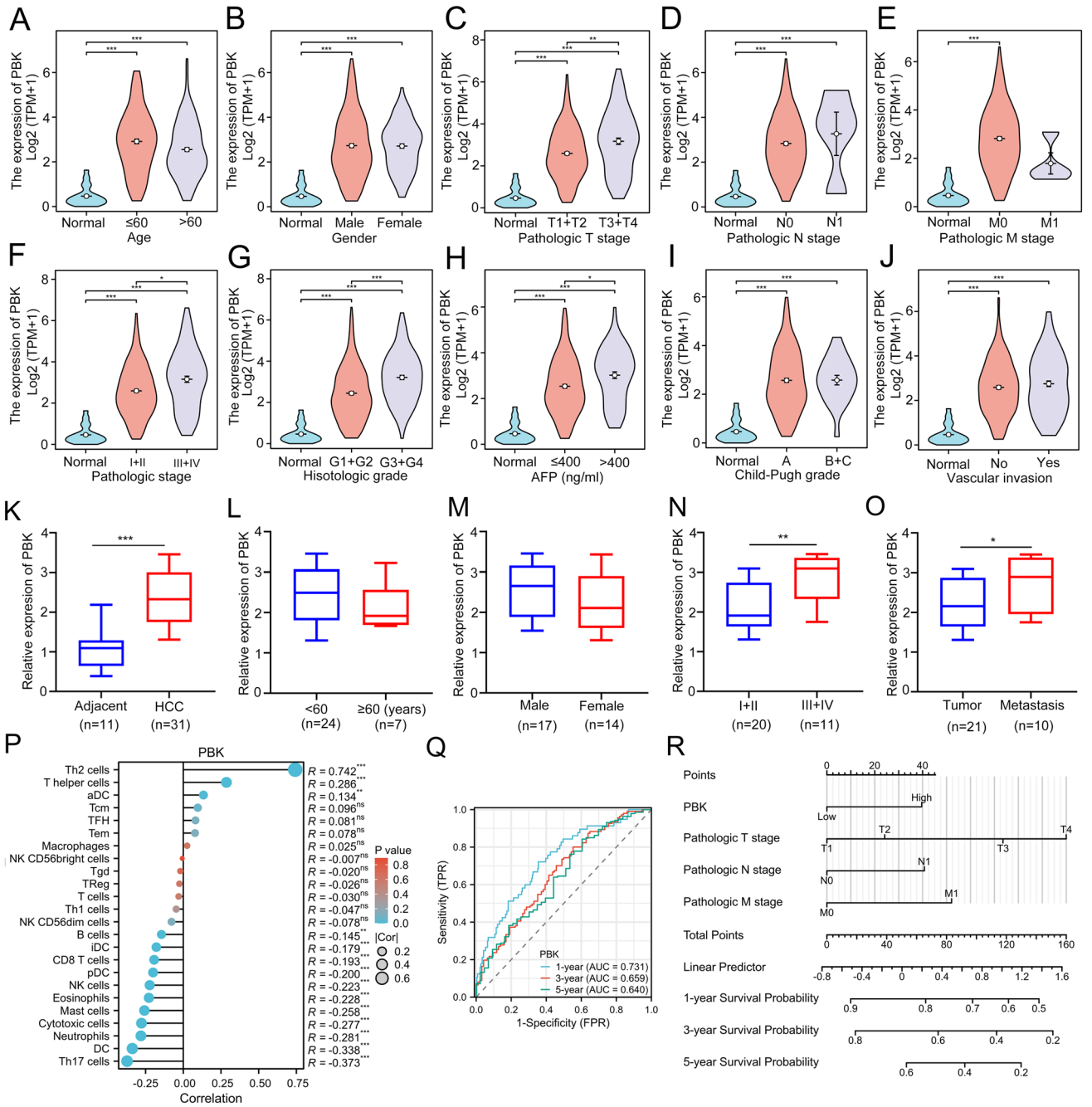

Fig. 4 PBK1 expression was correlated with the clinical features and prognosis of HCC. A, Expression of PBK in HCC with different ages. B, Expression of PBK in HCC with different genders. C, Expression of PBK in different T stage of tumor tissues. D, Expression of PBK in different N stage of HCC samples. E, Expression of PBK in different M stages of HCC tissues. F, Expression of PBK in different progressions of tumor. G, Expression of PBK in different histological stage of HCC. H, Expression of PBK in HCC with different AFP levels. I, Expression of PBK in HCC with different Child–Pugh grades. J, Expression of PBK in HCC with/without vascular invasion. K–O, Expression of PBK in HCC clinical samples (K) with different age (L), gender (M), stage (N) and metastasis status (O). P, The correlations between PBK expression and immune cell infiltrations. Q, ROC curve analysis if time-dependent survival to predict 1-, 3-, 5-year survival. R, A nomogram model combining clinicopathological factors and PBK expression to predict 1-, 3-, 5-year survival. HCC, hepatocellular carcinoma; ROC, receiver operator characteristic curve. $^{**}P < 0.01$, and $^{***}P < 0.001$

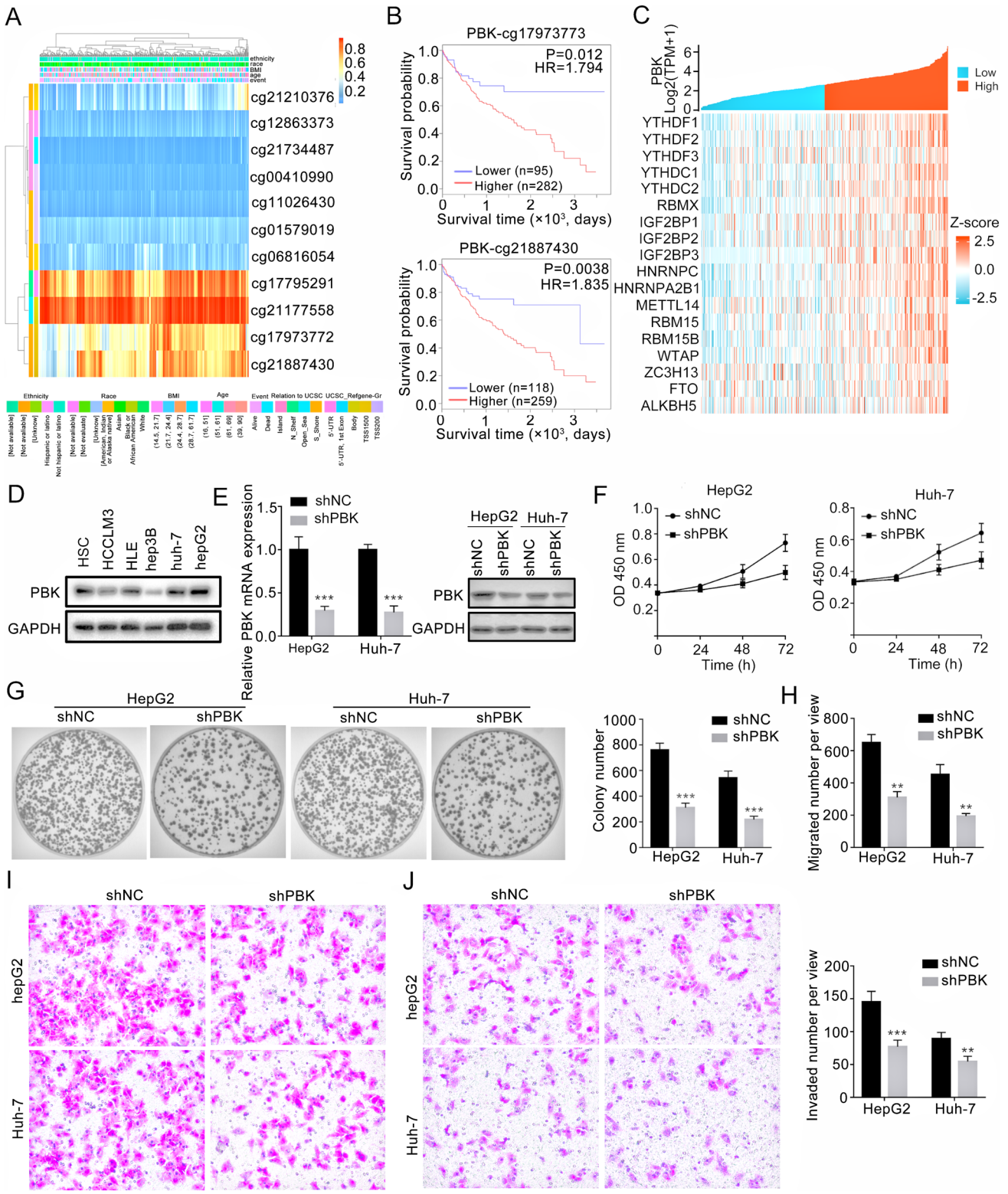

that dysregulated methylation might be an underlying cause for the upregulation of PBK in HCC.

To further confirm PBK in HCC, PBK expression was determined in HCC cell lines. The results suggested that PBK was significantly upregulated in HepG2 and Huh-7 cells (Fig. 5D). According to this, PBK was silenced in HepG2 and Huh-7 cells (Fig. 5E) followed by growth and metastasis analyses. CCK-8 and colony forming analysis

◂**Fig. 5** Dysregulated methylation-induced PBK upregulation promotes the growth and metastasis of HCC. A, The methylation sites of PBK in HCC. B, OS of cg17973773 and cg21887430 of PBK in HCC. C, Correlations between PBK expression and methylation associated proteins in HCC. D, Expression of PBK in HCC cell lines. E, Expression of PBK in HepG2 and Huh-7 cells after transfecting with shNC and shPBK determined using the qRT-PCR and western blotting. F, The proliferation of HepG2 and Huh-7 cells after transfecting with shNC and shPBK determined using CCK-8 assay. G, The colony formation ability of HepG2 and Huh-7 cells after transfecting with shNC and shPBK determined using colony formation assay. H and I, The migration ability of HepG2 and Huh-7 cells after transfecting with shNC and shPBK determined using transwell assay. J, The invasive ability of HepG2 and Huh-7 cells after transfecting with shNC and shPBK determined using transwell assay coated by Matrigel on membrane. NC, negative control; OS, overalll survival. $^{**}P<0.01$ compared with the control group, and $^{***}P<0.001$ compared with the control group

presented that silencing PBK significantly inhibited the proliferation and growth of HepG2 and Huh-7 cells (Fig. 5F and G). Further transwell assays showed that inhibiting PBK expression remarkably suppressed the migration and invasion abilities of HepG2 and Huh-7 (Fig. 5H–J). These findings suggested that targeting PBK significantly inhibited the progression of HCC.

Discussion

As one of the deadliest cancers, HCC exerts a challenging global health and huge economic burden worldwide. Early diagnosis and prognosis predicted are important to improve the outcome of HCC patients. In recent decade, rapid development of omics provided us more insights in understanding the diagnosis and treatment of HCC (Philips et al. 2021). However, clinical feature associated biomarkers are rarely reported in HCC. Considering of this, a clinical feature-based prognosis associated gene model was constructed in this study to provide a new candidate for the diagnosis and prognosis prediction of HCC. Among this model, upregulated PBK might play key roles in promoting the development of HCC via regulating the crosstalk between tumor cells and immune infiltrations among tumor microenvironment. The flowchart of this study was summarized in Supplementary Fig. 2.

Clinical features are a series of characteristics presented by patients, and are the direct evidence for disease progression. HCC is a highly heterogeneity cancer that appears morphological difference among patients with/without different treatments (Crocetti et al. 2017). For hepatitis B-associated HCC, patients received nucleoside analog (NUC) therapy presented more common single tumor nodule and lower portal vein invasion and metastasis than that without NUC treatment (Liu 2020). HCC patients complicated with bile duct invasion presented a poor prognosis than that without invasion, therefore aggressive treatment, including biliary drainage or resection might be beneficial treatment for them (An et al. 2017). Genes is the initial factor controlling the clinical presentation of cancers. For examples, HCC with higher expression of LOC90784 presented poor tumor differentiation stage, higher TNM stage and HBV status, as well as a poor OS rate than that individuals with low expression of LOC90784 (Xu et al. 2017). MCM6 was identified to promote the S/G2 cell cycle progression, and patients with higher MCM6 expression presented advanced TNM stage and a poor prognosis in patients with HCC (Liu et al. 2018). Considering of these evidences, we had combined the gene expression and clinical feature to constructed a 14-gene based prognosis associated gene model in this study, including *TRIP13*, *KIF4A*, *CENPA*, *CDCA8*, *CTSV*, *NUF2*, *SGOL2*, *PBK*, *BUB1*, *CBX2*, *UBE2C*, *IQGAP3*, *CDCA2*, and *KIF18B*. According to the clinical feature median in this model, the high-risk group presented a poor prognosis than the low-risk group according to the K-M analysis. Thus, we suspected that clinical feature-based gene set might be significantly correlated with the progression of HCC, and this model might be utilized for the diagnosis and prognosis prediction of HCC.

GO-BP enrichment analysis of the 14 genes showed that most of them were enriched in mitotic spindle assembly and kinetochore organization, which were all involved in chromatid segregation. Specifically, PBK, CDCA8, BUB1, and NUF2 were significantly enriched in cell cycle checkpoint, suggested that these four proteins played crucial roles in this signature regulation. NUF2, also known as CDCA1, was an important component of Ndc80/Nuf2 complex and had been upregulated in multiple cancers with poor prognosis, but the exact mechanism remains unclear (Jiang et al. 2021). Upregulated NUF2 was also identified in HCC and indicated a poor prognosis (Guo et al. 2020). Mechanism, NUF2 promoted the progression of HCC via stabilizing ERBB3 to active PI3K/Akt pathway (Liu et al. 2024). In addition, CDCA8 was also upregulated in HCC and facilitate HCC progression via activating CDK1/cyclin B1 signaling and AKT/β-catenin signaling (Jeon et al. 2021; Cui and Jiang 2024). BUB1 and PBK, also known as T-lymphokine-activated killer-cell-originated protein kinase (TOPK), were two mitotic checkpoint serine/threonine kinase that play crucial role in chromosomes partition (Han et al. 2021). Silencing BUB1 markedly reduced the proliferation and migration of HCC cells via inhibiting the phosphorylation of SMAD2 and SMAD3 (Qi et al. 2022). A previous study had documented that PBK was significantly upregulated in HCC and associated with the vascular invasion and poor prognosis of patients via enhancing uPAR and its downstream ETV4 expression (Yang et al. 2019). In this study, we had identified that BUB1, PBK, NUF, and CDCA8 were significantly upregulated in HCC and correlated with the 5-year OS of

HCC patients. In addition, all of them were presented excellent diagnostic values for HCC with all AUC more than 0.96. These findings suggested that BUB1, PBK, NUF, and CDCA8 played key regulative roles in this gene signature, and might be used for further HCC diagnostic and prognostic predictions, which remains required further confirmation.

Among the four key genes, PBK was the only independent risk factor for DSS of HCC. Clinical features analysis showed that higher PBK was significantly correlated with superior pathological stage and histological stages, as well as AFP, a recommended biomarker for HCC in the past. As a key checkpoint, abnormal activation of PBK had been reported in several cancers, and strongly correlated with the proliferation, progression, and metastasis of several cancers via regulating JNK, ERK, PI3K/PTEN/AKT, and p38 signaling pathways (Huang et al. 2021). He et al. had revealed that PBK, CDK1, RRM2, and ASPM might be the key genes in the transformation of cirrhosis to HCC (He et al. 2017). A recent study had revealed that PBK enhanced the drug resistance of HCC cells to oxaliplatin via PTEN mediating signaling pathway (Cao et al. 2021b). However, the upstream mechanism of PBK was rarely reported. In the current study, we had identified that cg17973772 and cg21887430 sites of PBK were obviously altered in HCC and higher expression of them were significantly correlated with the poor OS of HCC compared with the lower group. These findings suggested that dysregulation of methylation might be responsible for the upregulation of PBK in HCC, but the exact mechanism still required further confirmation.

Immune microenvironment is an essential component in the tumor microenvironment to promote the progression of tumors. In this study, we had identified that PBK was positively correlated with the infiltrations of Th2 cells and T helper cells, but negatively correlated with the infiltrations of B cells, CD8 + T cells, and Th17 cells. T cells and B cells are major component of adaptive immunity. Specifically, B cells are classical positive regulators to modulate immune response and inflammation via secreting antibodies and activating T cells (Shang et al. 2020). Previous study showed that B cells could inhibit T cell response in particular through the releasing of immunosuppressive cytokines. In human cancers, B cells density usually correlated with favorable prognosis and indicated therapeutic response to immune checkpoint inhibitors (ICIs) in tumor with low tumor burden (Fridman et al. 2020). IgA + B cells was identified to inhibit cytotoxic response of T cells, thereby inhibiting hepatocarcinogenesis in the inflamed liver (Shalapour et al. 2017). However in inflammation-driven HCC model, B cell-rich tertiary lymphoid structures (TLSs) could serve as a niche protecting tumor progenitor cells to facilitate growth of malignant cells via releasing lymphotoxin β (Finkin et al. 2015). Combined these findings, whether B cells served as double-edged sword in hepatocarcinogenesis or had been exhausted in HCC remains required further confirmations, as well as the role of PBK involved in this progression. NK, neutrophils, DC, mast cells, and eosinophils are all innate immune cells involving in tumor suppression by directly killing tumor cells or inducing adaptive immune response. Despite of these, several innate immune cells also contribute to the tumor progression and immunotherapy response insensitivity. This study had identified that PBK was also positively correlated with the infiltrations of aDC, while negatively correlated with the infiltrations of iDC, pDC, NK cells, eosinophils, mast cells, cytotoxic cells, neutrophils, and DC, indicating different subtypes of DCs played key roles in PBK-associated innate immune cells. DCs are the most potent antigen-presenting cells to activate innate immunity and enhancing cytotoxic activity of NKs and T lymphocyte-mediated adaptive immunity to eliminate tumor cells (Jeng et al. 2022). A recent study showed that blocking CD47 enhanced the antitumor efficacy of CD103 + DCs in HCC mice model (Wang et al. 2022). However, Pang et al. had revealed that tumor-derived extracellular adenosine might promoted pDC accumulation in HCC via adenosine A1 receptor to induce immunosuppression in HCC (Pang et al. 2021). These findings suggested that PBK functioned a key role in the progression of HCC via regulating the crosstalk among tumor cells and multiple immune associated cells. However, subtypes of immune cells might be more accuracy to explain the role of adaptive immune system in HCC.

There were still some limitations in this study. First, although a comprehensive prognosis associated gene model is identified in this study, the gene number might limit its application in clinic. Hence, it is of significance to simplify this gene model according to the clinical researches. Second, PBK was considered to be a hub gene in this gene model, but the crosstalk between PBK and other genes was not fully understood in HCC. Last but not the least, PBK had been predicted to play crucial roles in immune crosstalk of HCC, but the underlying mechanism in the progression of HCC still required further explorations.

In conclusion, a comprehensive prognosis associated 14-gene model was identified in this study based on the clinical features, which might be possible served as candidate for the diagnosis and prognosis of HCC. PBK, CDCA8, BUB1, and NUF2 might play key roles in these 14-gene/protein interaction, and presented excellent prediction values in the diagnosis and the 5-year OS of HCC. Among these four proteins, PBK was an independent risk factor for DSS of HCC and significantly correlated with the tumor stage and histological stage of HCC. Deregulated methylations might be responsible for the upregulation of PBK to promote the proliferation and metastasis of HCC via regulating the crosstalk between immune cells infiltrations and tumor cells. Thus, it is of importance to reveal the role of PBK, as well

as CDCA8, BUB1, and NUF2 in the progression of HCC, thereby promoting the diagnostic and prognostic predictions of HCC.

Supplementary Information The online version contains supplementary material available at https://doi.org/10.1007/s10735-024-10324-z.

Acknowledgements We acknowledged the Lab of Rajiv Kumar Jha Professor provide us the platform for experimental researches. We also acknowledge TCGA, STRING databased to providing their platforms for this study.

Authors' contributions Na He, Na Ye, and Beibei Lv conceived this study. Na Ye, and Beibei Lv performed the bioinformatics analyses. Fenna Zhang, Xinyi Zhang, Ziyi Wang, Shuai Hao performed the experiments and statistically analyses. Beibei Lv and Fenna Zhang wrote the manuscript. Na Ye and Na He revised the manuscript. All authors read and approved the final manuscript.

Funding This work was supported by grants from the Shaanxi Fundamental Science Research Project for Chemistry & Biology (Grant No. 22JHQ-091) and Shaanxi Provincial Natural Science Basic Research Program (Grant No. 2021JM-493).

Data availability No datasets were generated or analysed during the current study.

Declarations

Conflict of interests The authors declare no competing interests.

References

An J, Lee KS, Kim KM, Park DH, Lee SS, Lee D et al (2017) Clinical features and outcomes of patients with hepatocellular carcinoma complicated with bile duct invasion. Clini Mol Hepatol. https://doi.org/10.3350/cmh.2016.0088

Bian G, Cao J, Li W, Huang D, Ding X, Zang X et al (2024) Identification and validation of a cancer-testis antigen-related signature to predict the prognosis in stomach adenocarcinoma. J Cancer 15:3596

Cao W, Chen H-D, Yu Y-W, Li N, Chen W-Q (2021a) Changing profiles of cancer burden worldwide and in China: a secondary analysis of the global cancer statistics 2020. Chin Med J 134:783–791

Cao H, Yang M, Yang Y, Fang J, Cui Y (2021b) PBK/TOPK promotes chemoresistance to oxaliplatin in hepatocellular carcinoma cells by regulating PTEN. Acta Biochim Biophys Sin 53:584–592

Chalikonda G, Allen S, Vadde R, Nagaraju GP. Hepatocellular carcinoma diagnosis. Theranostics and precision medicine for the management of hepatocellular carcinoma, Volume 2: Elsevier; 2022. p. 1–5.

Chidambaranathan-Reghupaty S, Fisher PB, Sarkar D. Chapter One - Hepatocellular carcinoma (HCC): Epidemiology, etiology and molecular classification. In: Sarkar D, Fisher PB, editors. Advances in Cancer Research: Academic Press; 2021. p. 1–61.

Chumbley JR, Friston KJ (2009) False discovery rate revisited: FDR and topological inference using Gaussian random fields. Neuroimage 44:62–70

Crocetti L, Bargellini I, Cioni R (2017) Loco-regional treatment of HCC: current status. Clin Radiol 72:626–635

Cui Y, Jiang N (2024) CDCA8 facilitates tumor proliferation and predicts a poor prognosis in hepatocellular Carcinoma. Appl Biochem Biotechnol 196:1481–1492

Debes JD, Romagnoli PA, Prieto J, Arrese M, Mattos AZ, Boonstra A et al (2021) Serum biomarkers for the prediction of hepatocellular carcinoma. Cancers 13:1681

Finkin S, Yuan D, Stein I, Taniguchi K, Weber A, Unger K et al (2015) Ectopic lymphoid structures function as microniches for tumor progenitor cells in hepatocellular carcinoma. Nat Immunol 16:1235–1244

Fridman WH, Petitprez F, Meylan M, Chen TW-W, Sun C-M, Roumenina LT et al (2020) B cells and cancer: to B or not to B? J Exper Med. https://doi.org/10.1084/jem.20200851

Grinchuk OV, Yenamandra SP, Iyer R, Singh M, Lee HK, Lim KH et al (2018) Tumor-adjacent tissue co-expression profile analysis reveals pro-oncogenic ribosomal gene signature for prognosis of resectable hepatocellular carcinoma. Mol Oncol 12:89–113

Gui Z, Ye Y, Li Y, Ren Z, Wei N, Liu L et al (2024) Construction of a novel cancer-associated fibroblast-related signature to predict clinical outcome and immune response in cervical cancer. Trans Oncol 46:102001

Guo L, Wang Z, Du Y, Mao J, Zhang J, Yu Z et al (2020) Random-forest algorithm based biomarkers in predicting prognosis in the patients with hepatocellular carcinoma. Cancer Cell Int 20:251

Han Z, Li L, Huang Y, Zhao H, Luo Y (2021) PBK/TOPK: a therapeutic target worthy of attention. Cells 10:371

He B, Yin J, Gong S, Gu J, Xiao J, Shi W et al (2017) Bioinformatics analysis of key genes and pathways for hepatocellular carcinoma transformed from cirrhosis. Medicine 96:e6938

Huang H, Lee M-H, Liu K, Dong Z, Ryoo Z, Kim MO (2021) PBK/TOPK: an effective drug target with diverse therapeutic potential. Cancers 13:2232

Jeng L-B, Liao L-Y, Shih F-Y, Teng C-F (2022) Dendritic-cell-vaccine-based immunotherapy for hepatocellular carcinoma: clinical trials and recent preclinical studies. Cancers 14:4380

Jeon T, Ko MJ, Seo Y-R, Jung S-J, Seo D, Park S-Y et al (2021) Silencing CDCA8 suppresses hepatocellular carcinoma growth and stemness via restoration of ATF3 tumor suppressor and inactivation of AKT/β–catenin signaling. Cancers 13:1055

Jiang X, Jiang Y, Luo S, Sekar K, Koh CKT, Deivasigamani A et al (2021) Correlation of NUF2 overexpression with poorer patient survival in multiple Cancers. Cancer Res Treat 53:944–961

Lin J, Zhang H, Yu H, Bi X, Zhang W, Yin J et al (2022) Epidemiological characteristics of primary liver cancer in mainland China from 2003 to 2020: a representative multicenter study. Front Oncol 12:906778

Liu L (2020) Clinical features of hepatocellular carcinoma with hepatitis B virus among patients on Nucleos(t) ide analog therapy. Infect Agents Cancer 15:8

Liu Z, Li J, Chen J, Shan Q, Dai H, Xie H et al (2018) MCM family in HCC: MCM6 indicates adverse tumor features and poor outcomes and promotes S/G2 cell cycle progression. BMC Cancer 18:200

Liu Y, Wang Y, Wang J, Jiang W, Chen Y, Shan J et al (2024) NUF2 regulated the progression of hepatocellular carcinoma through modulating the PI3K/AKT pathway via stabilizing ERBB3. Trans Oncol 44:101933

Pang L, Ng KT-P, Liu J, Yeung W-HO, Zhu J, Chiu T-LS et al (2021) Plasmacytoid dendritic cells recruited by HIF-1α/eADO/ADORA1 signaling induce immunosuppression in hepatocellular carcinoma. Cancer Lett. https://doi.org/10.1016/j.canlet.2021.09.022

Philips CA, Rajesh S, Nair DC, Ahamed R, Abduljaleel JK, Augustine P. Hepatocellular carcinoma in 2021: an exhaustive update. Cureus. 2021;13

Pohar M, Stare J (2006) Relative survival analysis in R. Comput Methods Programs Biomed 81:272–278

Qi W, Bai Y, Wang Y, Liu L, Zhang Y, Yu Y et al (2022) BUB1 predicts poor prognosis and immune status in liver hepatocellular carcinoma. APMIS 130:371–382

Ritchie ME, Phipson B, Wu D, Hu Y, Law CW, Shi W et al (2015) limma powers differential expression analyses for RNA-sequencing and microarray studies. Nuclei Acids Res 43:e47

Ruf B, Heinrich B, Greten TF (2021) Immunobiology and immunotherapy of HCC: spotlight on innate and innate-like immune cells. Cell Mol Immunol 18:112–127

Ruppert D, Nettleton D, Hwang JG (2007) Exploring the information in p-values for the analysis and planning of multiple-test experiments. Biometrics 63:483–495

Shalapour S, Lin X-J, Bastian IN, Brain J, Burt AD, Aksenov AA et al (2017) Inflammation-induced IgA+ cells dismantle anti-liver cancer immunity. Nature 551:340–345

Shang J, Zha H, Sun Y (2020) Phenotypes, functions, and clinical relevance of regulatory B cells in Cancer. Front Immunol. https://doi.org/10.3389/fimmu.2020.582657

Sorop A, Constantinescu D, Cojocaru F, Dinischiotu A, Cucu D, Dima SO (2021) Exosomal microRNAs as biomarkers and therapeutic targets for hepatocellular carcinoma. Int J Mol Sci 22:4997

Villa E, Critelli R, Lei B, Marzocchi G, Cammà C, Giannelli G et al (2016) Neoangiogenesis-related genes are hallmarks of fast-growing hepatocellular carcinomas and worst survival. Results Prospect Study Gut 65:861–869

Vogel A, Martinelli E, Cervantes A, Chau I, Daniele B, Llovet J et al (2021) Updated treatment recommendations for hepatocellular carcinoma (HCC) from the ESMO clinical practice guidelines. Ann Oncol 32:801–805

Wang W, Wei C (2020) Advances in the early diagnosis of hepatocellular carcinoma. Genes & Diseases 7:308–319

Wang S, Wu Q, Chen T, Su R, Pan C, Qian J et al (2022) Blocking CD47 promotes antitumour immunity through CD103+ dendritic cell–NK cell axis in murine hepatocellular carcinoma model. J Hepatol 77:467–478

Xu J-H, Chang W-H, Fu H-W, Shu W-Q, Yuan T, Chen P (2017) Upregulated long non-coding RNA LOC90784 promotes cell proliferation and invasion and is associated with poor clinical features in HCC. Biochem Biophys Res Commun 490:920–926

Yang Q-X, Zhong S, He L, Jia X-J, Tang H, Cheng S-T et al (2019) PBK overexpression promotes metastasis of hepatocellular carcinoma via activating ETV4-uPAR signaling pathway. Cancer Lett 452:90–102

Zhao J, Wang Y, Su H, Su L (2021) Non-coding RNAs as biomarkers for hepatocellular carcinoma—a systematic review. Clin Res Hepatol Gastroenterol 45:101736